

RESEARCH

Open Access

Dual-hop MIMO relaying with OSTBC over doubly-correlated Nakagami- m fading channels

Kai Yang¹, Jie Yang^{2*} and Liyu Cai¹

Abstract

In this article, we investigate the performance of dual-hop amplify-and-forward multiple-input multiple-output relaying system with orthogonal space-time block code transmissions over doubly-correlated Nakagami- m fading channel, where the source, relay, and destination terminals are all equipped with multiple antennas. For two different CSI-assisted relaying schemes, which could be encompassed by a unified model, we provide the compact closed-form expressions for cumulative distribution function, probability density function, moment generating function, and generalized moment (GM) of the instantaneous end-to-end SNR. Besides, the exact analytical expressions for the outage probability (OP) and symbol error rate (SER) and approximate expression for ergodic capacity are also derived. Furthermore, we present the asymptotic expressions for OP and SER in the high SNR regime, from which we gain an insight into the system performance and derive the achievable diversity order and array gain. The analytical expressions are validated by Monte-Carlo simulations.

Keywords: Amplify-and-forward (AF) relaying, Multiple-input multiple-output (MIMO), Orthogonal space-time block code (OSTBC)

Introduction

Recently, relaying transmission has attracted great attention due to their considerable advantages over direct transmission, such as extending the coverage, increasing the reliability, and saving the power consumption [1-3], and has already been discussed as part of the LTE-Advanced study [4]. One of the most common relay protocols is amplify-and-forward (AF) (or non-regenerative) for its low complexity and cost-effectiveness. For dual-hop AF relaying with single-input single-output (SISO), its performance has been well studied over both Rayleigh [2,3] and Nakagami [5] channels.

Multiple-input multiple-output (MIMO) technology has also received a significant interest in the past decade for its significant increase in data throughput and link range without additional bandwidth or increased transmit power. Beamforming and space-time block code (STBC) techniques are two emerging technologies that

can be employed with multiple antennas to provide diversity.

In [6-8], the performance of two-hop relay network over correlated Rayleigh fading channels with beamforming [maximum ratio transmission (MRT) at the source and maximal ratio combining (MRC) at the destination] has been analyzed. In [9,10], the end-to-end performance of dual-hop relaying systems with beamforming over Nakagami- m fading channels has been investigated.

In [11-15], orthogonal space-time block code (OSTBC) has been employed in dual-hop relaying system. In [11,12], the end-to-end performance of dual-hop wireless communication systems employing transmit diversity with OSTBC over independent but not necessarily identically distributed (i.n.i.d.) Rayleigh and Nakagami- m fading channels has been well investigated respectively. Yan and Zhang [13] and Ferdinand et al. [14] extend the single-antenna relay in [11] to multiple-antenna relay over independent Rayleigh and asymmetric correlated Rayleigh-Rician fading channels, respectively. Yan and Zhang [13] have investigated the performance of a wireless relay network, where each of its nodes is equipped with N antennas and the same OSTBC scheme

*Correspondence: yangjie@bit.edu.cn

²School of Information and Electronics, Beijing Institute of Technology, Beijing, China

Full list of author information is available at the end of the article

is adopted at its source and relay nodes for transmission. In [14], the performance of MIMO AF relay network with OSTBC over Rayleigh-Rician asymmetric channel with antenna correlation has been analyzed. Duong et al. [15] extended i.n.i.d. Nakagami- m fading channels to arbitrarily correlated and not necessarily identically distributed (c.n.i.d.) Nakagami- m fading channels by transforming the sum of c.n.i.d. Gamma random variables (RVs) to a sum of independent Gamma RVs, where the relay is equipped with a single antenna.

Antenna correlation occurs in many practical scenarios due to the limited antenna separation or the lack of local scatters [16]. Louie et al. [6-8,15] only considered the one-sided correlated fading channels, where there was antenna correlation at either the transmitter or receiver. For a more general case of correlated fading at both the transmitter and receiver, which is referred to as doubly-correlated MIMO channels [17], it is important to quantify this correlation effect. In this article, we analyze the performance of two channel state information (CSI) assisted AF MIMO relaying systems over doubly-correlated Nakagami- m fading channels by building up the multiple-dimensional Gamma distributed correlated vector with order parameter m based on the sum of squared Gaussians [18], where all the source, relay, and destination terminals are equipped with multiple antennas and the channel fading at both transmission and reception ends is correlated with arbitrary correlation matrices. The source and relay terminals employ the OSTBC transmissions, which are not necessarily the same. It is noteworthy that it's easy to derive the performance of the dual-hop AF MIMO relaying system with OSTBC transmissions over doubly-correlated Rayleigh fading channels based on our analysis results, since the Nakagami- m distribution equals the Rayleigh distribution for $m = 1$. We assume that the instantaneous CSI is available at the relay terminal.

The rest of the article is organized as follows. The system and channel models studied are presented in Section "System and channel models". In Section "Metrics of end-to-end SNR", the compact closed-form expressions for the cumulative distribution function (CDF), probability density function (PDF), moment generating function (MGF), and generalized moment (GM) of the instantaneous end-to-end SNR are derived. In Section "Exact system performance analysis", the exact analytical expressions are also derived for the outage probability (OP) and symbol error rate (SER). In Section "Asymptotic analysis", the approximate expression for ergodic capacity is given firstly, and then the asymptotic expressions for OP and SER in the high SNR regime are presented. Numerical results that confirm our analysis are presented in Section "Numerical results", which is followed by the conclusion in Section "Conclusions".

System and channel models

Consider a dual-hop MIMO relaying network as shown in Figure 1. The source equipped with N_S antennas communicates with the destination equipped with N_D antennas via an N_R -antenna relay. Note that the results in the article can be easily extended to a more general case, where the relay uses different number of transmit and receive antennas. Under the assumption that the direct link between the source and destination is in deep fading, the direct link is ignored.

System model

We assume that the source and relay with multiple antennas employ OSTBC transmissions. An OSTBC with N_{Tx} transmission antennas is defined by an $N_{Tx} \times K$ transmission matrix \mathbf{X} , where K denotes the block length of an OSTBC and \mathbf{X} is constructed by a set of transmitted symbols x_l , $l = 1, \dots, L$. Since there is a total of L symbols transmitted over a period of K symbols, the code rate of OSTBCs is $R_c = L/K$.

During the first hop, the $N_R \times K_1$ signal matrix received at the relay could be written as

$$\mathbf{Y}_R = \mathbf{H}_1 \mathbf{X}_1 + \mathbf{N}_1, \quad (1)$$

where $\mathbf{H}_1 \in \mathbb{C}^{N_R \times N_S}$ denotes the spatially correlated Nakagami- m distributed channel matrix from the source to relay, $\mathbf{X}_1 \in \mathbb{C}^{N_S \times K_1}$ is the OSTBC codeword matrix with code rate $R_{c,1} = L/K_1$, and $\mathbf{N}_1 \in \mathbb{C}^{N_R \times K_1}$ is the noise matrix whose elements are independent and identically distributed (i.i.d.) complex Gaussian RVs with zero mean and variance $N_0/2$. OSTBC decouples the space-time channel into parallel scalar channels each with [19]

$$x_{R,l} = \|\mathbf{H}_1\|_F^2 x_l + \tilde{n}_{R,l}, \quad l = 1, \dots, L, \quad (2)$$

where the subscript F denotes the Frobenius norm, and $\tilde{n}_{R,l}$ is the filtered noise with zero mean and variance $\|\mathbf{H}_1\|_F^2 N_0$.

In the second hop, the output signal at the relay $x_{R,l}$ is amplified by the gain of the relay, G , encoded by an OSTBC matrix $\mathbf{X}_2 \in \mathbb{C}^{N_R \times K_2}$ with code rate $R_{c,2} = L/K_2$

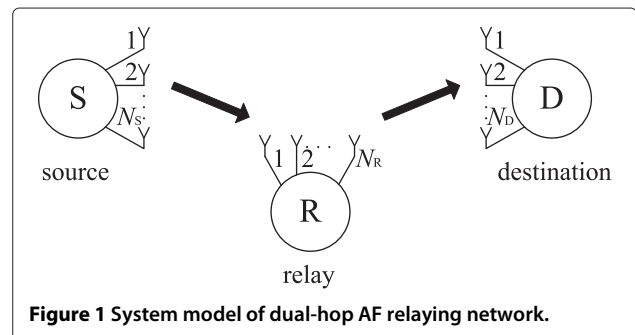


Figure 1 System model of dual-hop AF relaying network.

and then sent to the destination. The $N_D \times K_2$ signal matrix received at the destination could be written as

$$\mathbf{Y}_D = \mathbf{H}_2 \mathbf{X}_2 + \mathbf{N}_2, \quad (3)$$

where $\mathbf{H}_2 \in \mathbb{C}^{N_D \times N_R}$ denotes the spatially correlated Nakagami- m distributed channel matrix between the relay and destination, and $\mathbf{N}_2 \in \mathbb{C}^{N_D \times K_2}$ is the noise matrix whose elements are i.i.d. complex Gaussian RVs with zero mean and variance $N_0/2$. The combined signal $x_{D,l}$ at the destination could be given by

$$x_{D,l} = G \|\mathbf{H}_2\|_F^2 x_{R,l} + \tilde{n}_{D,l}, \quad l = 1, \dots, L, \quad (4)$$

where $\tilde{n}_{D,l}$ is the filtered noise with zero mean and variance $\|\mathbf{H}_2\|_F^2 N_0$.

Substituting (2) into (4) yields

$$x_{D,l} = G \|\mathbf{H}_1\|_F^2 \|\mathbf{H}_2\|_F^2 x_l + G \|\mathbf{H}_2\|_F^2 \tilde{n}_{R,l} + \tilde{n}_{D,l}. \quad (5)$$

Hence, the end-to-end SNR could be written as

$$\gamma = \frac{\frac{E_S}{N_0} \|\mathbf{H}_1\|_F^4 \|\mathbf{H}_2\|_F^2}{\|\mathbf{H}_1\|_F^2 \|\mathbf{H}_2\|_F^2 + \frac{1}{G^2}}, \quad (6)$$

where $E_S = E[|x_l|^2]$. It is clear from (6) that the choice of the relaying gain defines the equivalent end-to-end SNR of the dual-hop relaying system.

Usually, there are two choices for the gain G to normalize the received signal [2]

$$\begin{aligned} G_1 &= \sqrt{\frac{E_R}{\|\mathbf{H}_1\|_F^4 E_S + \|\mathbf{H}_1\|_F^2 N_0}}, \\ G_2 &= \sqrt{\frac{E_R}{\|\mathbf{H}_1\|_F^4 E_S}}, \end{aligned} \quad (7)$$

where $E_R = E[|x_{R,l}|^2]$. The two choices are referred as the channel noise assisted and channel assisted gains respectively [5], and could be encompassed by the unified model

$$G = \sqrt{\frac{E_R}{\|\mathbf{H}_1\|_F^4 E_S + \beta \|\mathbf{H}_1\|_F^2 N_0}}, \quad (8)$$

where β is equal to 0 or 1 corresponding to the channel assisted gain G_2 and channel noise assisted gain G_1 , respectively. By substituting (8) into (6), we have

$$\gamma = \frac{\gamma_1 \gamma_2}{\gamma_1 + \gamma_2 + \beta}, \quad (9)$$

where $\gamma_1 = \rho_1 \|\mathbf{H}_1\|_F^2$, $\rho_1 = E_S/N_0$, $\gamma_2 = \rho_2 \|\mathbf{H}_2\|_F^2$, and $\rho_2 = E_R/N_0$.

Channel model

The correlated channel matrix \mathbf{H}_i , $i = 1, 2$, can be factorized in the form [20]

$$\mathbf{H}_i = \mathbf{R}_{\text{Rx},i}^{\frac{1}{2}} \mathbf{H}_{\text{iid},i} \left(\mathbf{R}_{\text{Tx},i}^{\frac{1}{2}} \right)^T, \quad (10)$$

where $\mathbf{R}_{\text{Tx},i}$ and $\mathbf{R}_{\text{Rx},i}$ are the transmission and reception correlation matrices of i -th hop respectively, $\mathbf{H}_{\text{iid},i}$ is a matrix of i.i.d. RVs, and the superscript T denotes the matrix transpose operation. The entry of $\mathbf{R}_{\text{Tx},i}$ ($\mathbf{R}_{\text{Rx},i}$), $\rho_{\text{Tx},i}^{(j,k)}$ ($\rho_{\text{Rx},i}^{(j,k)}$), is the correlation coefficient between j -th and k -th transmission (reception) antennas of i -th hop. Based on the Kronecker product of the transmission and reception correlation matrices, we have

$$\text{vec}(\mathbf{H}_i) = \mathbf{R}_i^{\frac{1}{2}} \text{vec}(\mathbf{H}_{\text{iid},i}), \quad (11)$$

where $\text{vec}(\cdot)$ denotes the matrix vectorization operation, $\mathbf{R}_i = \mathbf{R}_{\text{Tx},i}^T \otimes \mathbf{R}_{\text{Rx},i}$, and \otimes denotes the Kronecker product.

By building up the multiple-dimensional Gamma distributed correlated vector with order parameter m based on the sum of squared Gaussians, the MGF of $\|\mathbf{H}_i\|_F^2$ could be given by [18]

$$\mathcal{M}_{\|\mathbf{H}_i\|_F^2}(s) = \left| \mathbf{I}_i + \frac{s}{m_i} \mathbf{D}_{\bar{\gamma},i} \mathbf{R}_i \right|^{-m_i}, \quad (12)$$

where m_i is the Nakagami- m fading parameter of i -th hop, \mathbf{I}_i is the identity matrix of size $N_{\text{Tx},i} \times N_{\text{Rx},i}$, $\mathbf{D}_{\bar{\gamma},i} = \text{diag}\{\bar{\gamma}_{i,1}, \bar{\gamma}_{i,2}, \dots, \bar{\gamma}_{i,N_{\text{Tx},i} \times N_{\text{Rx},i}}\}$, and $\bar{\gamma}_{i,j}$, $j = 1, \dots, N_{\text{Tx},i} \times N_{\text{Rx},i}$, is the average SNR for the j -th branch in $\text{vec}(\mathbf{H}_i)$. By using an eigenvalue factorization, the matrix $\mathbf{D}_{\bar{\gamma},i} \mathbf{R}_i$ can be diagonalized as

$$\mathbf{D}_{\bar{\gamma},i} \mathbf{R}_i = \mathbf{U}_i \Lambda_i \mathbf{U}_i^{-1}, \quad (13)$$

where

$$\Lambda_i = \text{diag}\{\lambda_{i,1}, \dots, \underbrace{\lambda_{i,j}, \dots, \lambda_{i,j}}_{v_{ij}}, \dots, \lambda_{i,J_i}\},$$

and $\lambda_{i,j}$, $j = 1, \dots, J_i$, is the distinct eigenvalue of $\mathbf{D}_{\bar{\gamma},i} \mathbf{R}_i$ with multiplicity v_{ij} such that $\sum_{j=1}^{J_i} v_{ij} = N_{\text{Tx},i} \times N_{\text{Rx},i}$. Substituting (13) into (12) yields

$$\mathcal{M}_{\|\mathbf{H}_i\|_F^2}(s) = \left| \mathbf{I}_i + \frac{s}{m_i} \Lambda_i \right|^{-m_i} = \prod_{j=1}^{J_i} \left(1 + \frac{s}{m_i} \lambda_{i,j} \right)^{-m_i v_{ij}}. \quad (14)$$

In particular, for the case of balanced branches, i.e. $\bar{\gamma}_{i,1} = \bar{\gamma}_{i,2} = \dots = \bar{\gamma}_{i,N_{\text{Tx},i} \times N_{\text{Rx},i}}$, (12) can be expressed in terms of the eigenvalues associated with \mathbf{R}_i as follows:

$$\mathcal{M}_{\|\mathbf{H}_i\|_F^2}(s) = \prod_{j=1}^{J_i} \left(1 + \frac{s \bar{\gamma}_{i,1}}{m_i} \phi_{i,j} \right)^{-m_i u_{i,j}}, \quad (15)$$

where $\phi_{i,j}$, $j = 1, \dots, J_i$, denotes the distinct eigenvalue of \mathbf{R}_i with multiplicity $u_{i,j}$ such that $\sum_{j=1}^{J_i} u_{i,j} = N_{\text{Tx},i} \times N_{\text{Rx},i}$, and is the product of the eigenvalues of $\mathbf{R}_{\text{Tx},i}$ and $\mathbf{R}_{\text{Rx},i}$.

By expanding in poles and residuals, (14) can be decomposed into the following partial fractions ([21], eq. (2.102))

$$\mathcal{M}_{\|\mathbf{H}_i\|_F^2}(s) = \sum_{j=1}^{J_i} \sum_{k=1}^{m_i v_{ij}} c_{j,k}^i \left(1 + \frac{s}{m_i} \lambda_{ij}\right)^{-k}, \quad (16)$$

where

$$c_{j,k}^i = \frac{1}{(m_i v_{ij} - k)!} \left(\frac{m_i}{\lambda_{ij}}\right)^{m_i v_{ij} - k} \frac{d^{m_i v_{ij} - k}}{ds^{m_i v_{ij} - k}} \left(\mathcal{M}_{\|\mathbf{H}_i\|_F^2}(s) \left(1 + \frac{s}{m_i} \lambda_{ij}\right)^{m_i v_{ij}} \right) \Big|_{s = -\frac{m_i}{\lambda_{ij}}}.$$

From the relationship between MGF and PDF, based on the linearity of the inverse of the Laplace transform and the identity for inverse Laplace transformation, given in ([22], eq. (5.2.17)), we could therefore write for the PDF of $\|\mathbf{H}_i\|_F^2 = z$, where $z > 0$, as

$$f(z) = \sum_{j=1}^{J_i} \sum_{k=1}^{m_i v_{ij}} c_{j,k}^i \left(\frac{\lambda_{ij}}{m_i}\right)^{-k} \frac{z^{k-1}}{\Gamma(k)} \exp\left(-\frac{m_i z}{\lambda_{ij}}\right), \quad (17)$$

where $\Gamma(\cdot)$ is the gamma function defined as $\Gamma(x) = \int_0^\infty t^{x-1} e^{-t} dt$ [21].

By integrating the PDF with respect to z with the help of ([21], eq. (3.351.1)), the CDF of z could be given by

$$F(z) = 1 - \sum_{j=1}^{J_i} \sum_{k=1}^{m_i v_{ij} - 1} \sum_{l=0}^{k-1} \frac{c_{j,k}^i}{l!} \exp\left(-\frac{m_i z}{\lambda_{ij}}\right) \left(\frac{m_i z}{\lambda_{ij}}\right)^l, \quad (18)$$

where the above deduction uses the property of $\sum_{j=1}^{J_i} \sum_{k=1}^{m_i v_{ij}} c_{j,k}^i = 1$, which can be derived by substituting $s = 0$ into (12) and (16) and comparing the results.

Metrics of end-to-end SNR

In this section, the compact closed-form expressions for CDF of the end-to-end SNR γ are presented firstly. Then the exact analytical expressions for the PDE, MGF, and GM of γ are derived relying on CDF.

CDF of γ

The CDF of end-to-end SNR γ could be written as

$$F_\gamma(\gamma) = 1 - 2 \sum_{j=1}^{J_1} \sum_{k=1}^{m_1 v_{1j}} \sum_{l=0}^{k-1} \sum_{p=1}^{J_2} \sum_{q=1}^{m_2 v_{2p}} \sum_{g=0}^{q-1} \times \sum_{h=0}^l \binom{q-1}{g} \binom{l}{h} \frac{c_{j,k}^1 c_{p,q}^2}{\Gamma(l+1) \Gamma(q)} \times \left(\frac{m_1}{\rho_1 \lambda_{1j}}\right)^{\frac{\theta+1}{2}} \left(\frac{\rho_2 \lambda_{2,p}}{m_2}\right)^{\frac{\theta-1}{2}-q} \times \exp\left(-\frac{m_1 \gamma}{\rho_1 \lambda_{1j}} - \frac{m_2 \gamma}{\rho_2 \lambda_{2,p}}\right) \times \gamma^{-\frac{g+h+l-1}{2}+q} (\gamma + \beta)^{\frac{g-h+l+1}{2}} K_{\theta-l}(2\gamma'), \quad (19)$$

where $\gamma' = \sqrt{\frac{m_1 m_2 \gamma (\gamma + \beta)}{\rho_1 \lambda_{1j} \rho_2 \lambda_{2,p}}}$, $\theta = g + h + 1$, and $K_\nu(\cdot)$ denotes the ν th-order modified Bessel function of the second kind.

Proof. The proof is provided in Appendix 1. \square

PDF of γ

The close-form expression for the PDF of γ can be given by

$$f_\gamma(\gamma) = 2 \sum_{j=1}^{J_1} \sum_{k=1}^{m_1 v_{1j}} \sum_{l=0}^{k-1} \sum_{p=1}^{J_2} \sum_{q=1}^{m_2 v_{2p}} \sum_{g=0}^{q-1} \times \sum_{h=0}^l \binom{q-1}{g} \binom{l}{h} \frac{c_{j,k}^1 c_{p,q}^2}{\Gamma(l+1) \Gamma(q)} \left(\frac{m_1}{\rho_1 \lambda_{1j}}\right)^{\frac{\theta+1}{2}} \times \left(\frac{\rho_2 \lambda_{2,p}}{m_2}\right)^{\frac{\theta-1}{2}-q} \times \exp\left(-\frac{m_1 \gamma}{\rho_1 \lambda_{1j}} - \frac{m_2 \gamma}{\rho_2 \lambda_{2,p}}\right) \times \gamma^{-\frac{g+h+l-3}{2}+q} (\gamma + \beta)^{\frac{g-h+l-1}{2}} \times (\gamma' (2\gamma + \beta) K_{\theta-l+1}(2\gamma') + \varphi K_{\theta-l}(2\gamma')), \quad (20)$$

where $\varphi = \left(\frac{m_1}{\rho_1 \lambda_{1j}} + \frac{m_2}{\rho_2 \lambda_{2,p}}\right) \gamma (\gamma + \beta) - (\theta + q) \gamma - (h + q) \beta$.

Proof. Taking the derivative of (19) with respect to γ and using the expression for the derivative of the modified Bessel function, given in ([21], eq. (8.486.13)), yields (20). \square

MGF of γ

Moment generating function is useful in evaluating the system performance over fading channels. The MGF of γ can be presented as

$$\mathcal{M}_\gamma(s) = 1 - s \sum_{j=1}^{J_1} \sum_{k=1}^{m_1 v_{1j}} \sum_{l=0}^{k-1} \sum_{p=1}^{J_2} \sum_{q=1}^{m_2 v_{2p}} \sum_{g=0}^{q-1} \sum_{h=0}^l \times \sum_{\mu=0}^{g+l+2} \binom{q-1}{g} \binom{l}{h} \binom{g+l+2}{\mu} \times \frac{c_{j,k}^1 c_{p,q}^2 \Gamma(\theta+1)}{\Gamma(q) \beta^{\mu+h+1} (-1)^{q-g+\mu-1}} \left(\frac{\rho_1 \lambda_{1j}}{m_1}\right) \left(\frac{\rho_2 \lambda_{2,p}}{m_2}\right)^{\theta-q+1} \times \frac{d^{q-g+\mu-1}}{d\tilde{s}^{q-g+\mu-1}} ({}_2F_0(\theta+1, l+1; -\omega(\tilde{s} + \tilde{s}')) \times {}_2F_0(\theta+1, l+1; -\omega(\tilde{s} - \tilde{s}')) \Big|_{\tilde{s}=\tilde{s}'}, \quad (21)$$

where $\tilde{s}' = \sqrt{\tilde{s}^2 - \frac{2}{\beta\omega}}$, $\omega = \frac{\rho_1 \lambda_{1j} \rho_2 \lambda_{2,p}}{2\beta m_1 m_2}$, $\tilde{s}' = s + \frac{m_1}{\rho_1 \lambda_{1j}} + \frac{m_2}{\rho_2 \lambda_{2,p}}$, and ${}_2F_0(a, b; z)$ denotes the generalized hypergeometric function.

Proof. The proof is provided in Appendix 2. \square

Although (21) appears complicated, it is in closed form since higher order derivatives of arbitrary order are known for the generalized hypergeometric function ${}_pF_q((a_p);(b_q);z)$ [23]. Having the MGF in closed form as in (21) and using the MGF-based approach for the performance evaluation of digital modulations over fading channels [24], the average bit and SERs for some types of modulation can be derived from the MGF of the instantaneous fading SNR directly (e.g., differentially coherent detection of phase-shift-keying (PSK) or non-coherent detection of orthogonal frequency-shift-keying (FSK)).

For $\beta = 0$, (21) reduces to

$$\begin{aligned} \mathcal{M}_\gamma(s) &= 1 - 2s \sum_{j=1}^{J_1} \sum_{k=1}^{m_1 v_{1,j} k-1} \sum_{l=0}^{J_2} \sum_{p=1}^{m_2 v_{2,p} q-1} \sum_{q=1}^l \sum_{g=0}^{q-1} \binom{q-1}{g} \binom{l}{h} \\ &\times \frac{c_{j,k}^1 c_{p,q}^2}{\Gamma(l+1)\Gamma(q)} \left(\frac{m_1}{\rho_1 \lambda_{1,j}}\right)^{\frac{\theta+l}{2}} \left(\frac{\rho_2 \lambda_{2,p}}{m_2}\right)^{\frac{\theta-l}{2}-q} \\ &\times \frac{\sqrt{\pi}(2\varpi)^{\theta-l}}{(s'+\varpi)^{\theta+q+1}} \frac{\Gamma(\theta+q+1)\Gamma(2l+q-g-h)}{\Gamma(l+q+\frac{3}{2})} \\ &\times {}_2F_1\left(\theta+q+1, \theta-l+\frac{1}{2}; l+q+\frac{3}{2}; \frac{s'-\varpi}{s'+\varpi}\right), \end{aligned} \quad (22)$$

where $\varpi = 2\sqrt{\frac{m_1 m_2}{\rho_1 \lambda_{1,j} \rho_2 \lambda_{2,p}}}$.

Proof. By setting $\beta = 0$, (43) can be reduced to a manipulable form. By performing some algebraic manipulations with the help of expression for the definite integral of Bessel function, given in ([21], eq. (6.621.3)), the MGF of γ with $\beta = 0$ can be derived as shown in (22). \square

GM of γ

We now derive the GMs of γ that can efficiently be applied to uncover other statistical measures of the system performance. For instance, the average SNR, amount of fading, and ergodic capacity can be evaluated with the first-order and second-order moments.

The GM of γ can be expressed as

$$\begin{aligned} E(\gamma^n) &= n \sum_{j=1}^{J_1} \sum_{k=1}^{m_1 v_{1,j} k-1} \sum_{l=0}^{J_2} \sum_{p=1}^{m_2 v_{2,p} q-1} \sum_{q=1}^l \sum_{g=0}^{q-1} \sum_{h=0}^l \\ &\times \sum_{\mu=0}^{g+l+2} \binom{q-1}{g} \binom{l}{h} \binom{g+l+2}{\mu} \\ &\times \frac{c_{j,k}^1 c_{p,q}^2 \Gamma(\theta+1)}{\Gamma(q) \beta^{\mu+h+1} (-1)^{q-g+\mu+n-2}} \left(\frac{\rho_1 \lambda_{1,j}}{m_1}\right) \\ &\times \left(\frac{\rho_2 \lambda_{2,p}}{m_2}\right)^{\theta-q+1} \times \frac{d^{q-g+\mu+n-2}}{d\tilde{s}^{q-g+\mu+n-2}} \end{aligned}$$

$$\begin{aligned} &\times ({}_2F_0(\theta+1, l+1; ; -\omega\tilde{s}_+) \\ &\times {}_2F_0(\theta+1, l+1; ; -\omega\tilde{s}_-)) \Big|_{\tilde{s}=\frac{m_1}{\rho_1 \lambda_{1,j}} + \frac{m_2}{\rho_2 \lambda_{2,p}}}, \end{aligned} \quad (23)$$

where $\tilde{s}_+ = \tilde{s} + \sqrt{\tilde{s}^2 - \frac{4m_1 m_2}{\rho_1 \lambda_{1,j} \rho_2 \lambda_{2,p}}}$, and $\tilde{s}_- = \tilde{s} - \sqrt{\tilde{s}^2 - \frac{4m_1 m_2}{\rho_1 \lambda_{1,j} \rho_2 \lambda_{2,p}}}$.

Proof. The GM of γ can be obtained from

$$E(\gamma^n) = n \int_0^\infty \gamma^{n-1} (1 - F_\gamma(\gamma)) d\gamma. \quad (24)$$

By substituting (19) into (24) and performing the similar algebraic manipulations as in Appendix 2, the closed-form expression for GM of γ can be derived as shown in (23). \square

For $\beta = 0$, (23) deduces to

$$\begin{aligned} E(\gamma^n) &= 2n \sum_{j=1}^{J_1} \sum_{k=1}^{m_1 v_{1,j} k-1} \sum_{l=0}^{J_2} \sum_{p=1}^{m_2 v_{2,p} q-1} \sum_{q=1}^l \sum_{g=0}^{q-1} \\ &\times \sum_{h=0}^l \binom{q-1}{g} \binom{l}{h} \frac{c_{j,k}^1 c_{p,q}^2}{\Gamma(l+1)\Gamma(q)} \left(\frac{m_1}{\rho_1 \lambda_{1,j}}\right)^{\frac{\theta+l}{2}} \\ &\times \left(\frac{\rho_2 \lambda_{2,p}}{m_2}\right)^{\frac{\theta-l}{2}-q} \times \frac{\sqrt{\pi}(2\varpi)^{\theta-l}}{\left(\frac{m_1}{\rho_1 \lambda_{1,j}} + \frac{m_2}{\rho_2 \lambda_{2,p}} + \varpi\right)^{\theta+n+q}} \\ &\times \frac{\Gamma(\theta+n+q)\Gamma(2l+n+q-\theta)}{\Gamma(l+n+q+\frac{1}{2})} \times {}_2F_1 \\ &\times \left(\theta+n+q, \theta-l+\frac{1}{2}; l+n+q+\frac{1}{2}; \left(\frac{m_1}{\rho_1 \lambda_{1,j}} + \frac{m_2}{\rho_2 \lambda_{2,p}} - \varpi\right) / \left(\frac{m_1}{\rho_1 \lambda_{1,j}} + \frac{m_2}{\rho_2 \lambda_{2,p}} + \varpi\right)\right). \end{aligned} \quad (25)$$

Proof. Substituting (19) with $\beta = 0$ into (24) and performing some algebraic manipulations with the help of expression for the definite integral of Bessel function, given in ([21], eq. (6.621.3)), the GM of γ with $\beta = 0$ can be derived as shown in (25). \square

Exact system performance analysis

In this section, the exact analytical expressions are derived for the OP and SER based on the expressions presented in last section.

Outage probability

The OP is an important quality of service measure, which is defined as the probability that the instantaneous end-to-end SNR falls below a predetermined threshold γ_{th} and could be given by

$$P_{out} = P(\gamma < \gamma_{th}) = F_\gamma(\gamma_{th}), \quad (26)$$

where $F_\gamma(\gamma_{th})$ is the CDF of γ evaluated at $\gamma = \gamma_{th}$. Consequently, the OP could be evaluated by substituting (19) into (26).

Symbol error rate

With the aid of $\mathcal{M}_\gamma(s)$ presented in Section “MGF of γ ”, the average SER of some types of modulation can be easily obtained via the unified MGF-based approach [24]. However, for some cases (e.g., coherent detection of M-PSK, M-FSK, and M-QAM), the intractability arises in seeking a closed-form solution to the finite-range integration of the MGF expressions, which involve the generalized hypergeometric function.

In this section, we adopt an alternative approach to give the closed-form expression for SER directly in terms of the CDF of γ as [25]

$$P_s = \frac{a}{2} \sqrt{\frac{b}{\pi}} \int_0^\infty \frac{F(\gamma)}{\sqrt{\gamma}} \exp(-b\gamma) d\gamma, \quad (27)$$

where the parameters a and b are up to a specific modulation scheme to be used, e.g., for BPSK, $a = b = 1$.

For mathematical tractability, we set $\beta = 0$. Substituting (19) into (27), and performing some algebraic manipulations with the help of the expression for the definite integral of Bessel function, given in ([21], eq. (6.621.3)), yields

$$\begin{aligned} P_s &= \frac{a}{2} - a\sqrt{b} \sum_{j=1}^{J_1} \sum_{k=1}^{m_1 v_{1,j} k-1} \sum_{l=0}^{J_2} \sum_{p=1}^{m_2 v_{2,p} q-1} \sum_{q=1}^{m_2 v_{2,p} q-1} \sum_{g=0}^l \sum_{h=0}^l \binom{q-1}{g} \binom{l}{h} \\ &\times \frac{c_{j,k}^1 c_{p,q}^2}{\Gamma(l+1)\Gamma(q)} \left(\frac{m_1}{\rho_1 \lambda_{1,j}}\right)^{\frac{\theta+l}{2}} \left(\frac{\rho_2 \lambda_{2,p}}{m_2}\right)^{\frac{\theta-l}{2}-q} \\ &\times \frac{(2\varpi)^{\theta-l} \Gamma(\theta+q+\frac{1}{2}) \Gamma(2l+q+\frac{1}{2}-\theta)}{(\tilde{b}+\varpi)^{\theta+q+\frac{1}{2}} \Gamma(l+q+1)} \\ &\times {}_2F_1\left(\theta+q+\frac{1}{2}, \theta-l+\frac{1}{2}; l+q+1; \frac{\tilde{b}-\varpi}{\tilde{b}+\varpi}\right), \end{aligned} \quad (28)$$

where $\tilde{b} = b + \frac{m_1}{\rho_1 \lambda_{1,j}} + \frac{m_2}{\rho_2 \lambda_{2,p}}$.

Asymptotic analysis

In this section, the approximate expression for ergodic capacity is given firstly. The asymptotic expressions for OP and SER in high SNR regime are then derived in order to gain insight into the system performance, and the achievable diversity order and array gain of the relaying system are also presented.

Ergodic capacity

The ergodic capacity is determined by the expected value of the instantaneous mutual information between the

source and destination, which could be expressed in a second-order approximation as [26]

$$C_{\text{erg}} \approx \frac{\log_2(e)}{2} \left(\ln(1 + E(\gamma)) - \frac{E(\gamma^2) - E^2(\gamma)}{2(1 + E(\gamma))^2} \right). \quad (29)$$

By substituting $n = 1$ and $n = 2$ into (25), we have

$$\begin{aligned} E(\gamma) &= 2 \sum_{j=1}^{J_1} \sum_{k=1}^{m_1 v_{1,j} k-1} \sum_{l=0}^{J_2} \sum_{p=1}^{m_2 v_{2,p} q-1} \sum_{q=1}^{m_2 v_{2,p} q-1} \sum_{g=0}^l \sum_{h=0}^l \binom{q-1}{g} \binom{l}{h} \\ &\times \frac{c_{j,k}^1 c_{p,q}^2}{\Gamma(l+1)\Gamma(q)} \left(\frac{m_1}{\rho_1 \lambda_{1,j}}\right)^{\frac{\theta+l}{2}} \left(\frac{\rho_2 \lambda_{2,p}}{m_2}\right)^{\frac{\theta-l}{2}-q} \\ &\times \frac{\sqrt{\pi} (2\varpi)^{\theta-l}}{\left(\frac{m_1}{\rho_1 \lambda_{1,j}} + \frac{m_2}{\rho_2 \lambda_{2,p}} + \varpi\right)^{\theta+q+1}} \\ &\times \frac{\Gamma(\theta+q+1) \Gamma(2l+q-\theta+1)}{\Gamma(l+q+\frac{3}{2})} \\ &\times {}_2F_1\left(\theta+q+1, \theta-l+\frac{1}{2}; l+q+\frac{3}{2}; \left(\frac{m_1}{\rho_1 \lambda_{1,j}} + \frac{m_2}{\rho_2 \lambda_{2,p}} - \varpi\right) / \left(\frac{m_1}{\rho_1 \lambda_{1,j}} + \frac{m_2}{\rho_2 \lambda_{2,p}} + \varpi\right)\right). \end{aligned} \quad (30)$$

$$\begin{aligned} E(\gamma^2) &= 4 \sum_{j=1}^{J_1} \sum_{k=1}^{m_1 v_{1,j} k-1} \sum_{l=0}^{J_2} \sum_{p=1}^{m_2 v_{2,p} q-1} \sum_{q=1}^{m_2 v_{2,p} q-1} \sum_{g=0}^l \sum_{h=0}^l \binom{q-1}{g} \binom{l}{h} \\ &\times \frac{c_{j,k}^1 c_{p,q}^2}{\Gamma(l+1)\Gamma(q)} \left(\frac{m_1}{\rho_1 \lambda_{1,j}}\right)^{\frac{\theta+l}{2}} \left(\frac{\rho_2 \lambda_{2,p}}{m_2}\right)^{\frac{\theta-l}{2}-q} \\ &\times \frac{\sqrt{\pi} (2\varpi)^{\theta-l}}{\left(\frac{m_1}{\rho_1 \lambda_{1,j}} + \frac{m_2}{\rho_2 \lambda_{2,p}} + \varpi\right)^{\theta+q+2}} \\ &\times \frac{\Gamma(\theta+q+2) \Gamma(2l+q-\theta+2)}{\Gamma(l+q+\frac{5}{2})} \\ &\times {}_2F_1\left(\theta+q+2, \theta-l+\frac{1}{2}; l+q+\frac{5}{2}; \left(\frac{m_1}{\rho_1 \lambda_{1,j}} + \frac{m_2}{\rho_2 \lambda_{2,p}} - \varpi\right) / \left(\frac{m_1}{\rho_1 \lambda_{1,j}} + \frac{m_2}{\rho_2 \lambda_{2,p}} + \varpi\right)\right). \end{aligned} \quad (31)$$

Obviously, we can evaluate the ergodic capacity of the MIMO relaying systems by substituting (30) and (31) into (29).

Outage probability

By using Taylor series expansion of the exponential function at z equal to zero, from (18), we have

$$F(z) = 1 - \sum_{j=1}^{J_i} \sum_{k=1}^{m_i v_{i,j} k-1} \sum_{l=0}^{\infty} \frac{(-1)^l c_{j,k}^l}{l! l!} \left(\frac{m_i z}{\lambda_{i,j}} \right)^{l+t}$$

$$= D_i z^{N_{Tx,i} N_{Rx,i} m_i} + o\left(z^{N_{Tx,i} N_{Rx,i} m_i + 1}\right), \quad (32)$$

where

$$D_i = \sum_{j=1}^{J_i} \sum_{k=1}^{m_i v_{i,j} k-1} \sum_{l=0}^{\infty} \binom{N_{Tx,i} N_{Rx,i} m_i}{l} \frac{c_{j,k}^l \left(-\frac{m_i}{\lambda_{i,j}}\right)^{N_{Tx,i} N_{Rx,i} m_i}}{(N_{Tx,i} N_{Rx,i} m_i)! (-1)^{l-1}}.$$

Hence, the asymptotic expression for OP at high SNR can be written as [27]

$$P_{\text{out}}^{\infty} = \begin{cases} D_1 \left(\frac{\gamma_{\text{th}}}{\rho_1}\right)^{\tilde{m}_1} + o\left(\left(\frac{\gamma_{\text{th}}}{\rho_1}\right)^{\tilde{m}_1+1}\right), & \tilde{m}_1 < \tilde{m}_2 \\ D_2 \left(\frac{\gamma_{\text{th}}}{\rho_1}\right)^{\tilde{m}_2} + o\left(\left(\frac{\gamma_{\text{th}}}{\rho_1}\right)^{\tilde{m}_2+1}\right), & \tilde{m}_1 > \tilde{m}_2 \\ (D_1 + D_2) \left(\frac{\gamma_{\text{th}}}{\rho_1}\right)^{\tilde{m}_1} + o\left(\left(\frac{\gamma_{\text{th}}}{\rho_1}\right)^{\tilde{m}_1+1}\right), & \tilde{m}_1 = \tilde{m}_2 \end{cases} \quad (33)$$

where

$$D_1 = \sum_{j=1}^{J_1} \sum_{k=1}^{m_1 v_{1,j} k-1} \sum_{l=0}^{\infty} \binom{\tilde{m}_1}{l} \frac{c_{j,k}^1 \left(-\frac{m_1}{\lambda_{1,j}}\right)^{\tilde{m}_1}}{(\tilde{m}_1)! (-1)^{l-1}},$$

$$D_2 = \sum_{j=1}^{J_2} \sum_{k=1}^{m_2 v_{2,j} k-1} \sum_{l=0}^{\infty} \binom{\tilde{m}_2}{l} \frac{c_{j,k}^2 \left(-\frac{m_2}{\kappa \lambda_{2,j}}\right)^{\tilde{m}_2}}{(\tilde{m}_2)! (-1)^{l-1}},$$

and $\tilde{m}_1 = N_S N_{R1} m_1$, $\tilde{m}_2 = N_R N_D m_2$, $\kappa = \rho_2 / \rho_1$.

It should be noted that the value of β has no impact on the asymptotic expression of OP in high SNR regime.

Symbol error rate

Based on the relationship between CDF and OP, substituting (33) into (27) and after some algebraic manipulations with the help of definite integral of exponential function, given in ([21], eq. (3.381.10)), the asymptotic SER can be derived as [10,28]

$$P_s^{\infty} = (G_d \rho_1)^{-G_d} + o\left(\rho_1^{-G_d}\right), \quad (34)$$

where the diversity order G_d is

$$G_d = \min\{\tilde{m}_1, \tilde{m}_2\}, \quad (35)$$

and the array gain G_a is

$$G_a = \begin{cases} b \left(\frac{a D_1}{2\sqrt{\pi}} \Gamma\left(\tilde{m}_1 + \frac{1}{2}\right) \right)^{-\frac{1}{\tilde{m}_1}}, & \tilde{m}_1 < \tilde{m}_2 \\ b \left(\frac{a D_2}{2\sqrt{\pi}} \Gamma\left(\tilde{m}_2 + \frac{1}{2}\right) \right)^{-\frac{1}{\tilde{m}_2}}, & \tilde{m}_1 > \tilde{m}_2 \\ b \left(\frac{a (D_1 + D_2)}{2\sqrt{\pi}} \Gamma\left(\tilde{m}_1 + \frac{1}{2}\right) \right)^{-\frac{1}{\tilde{m}_1}}, & \tilde{m}_1 = \tilde{m}_2 \end{cases} \quad (36)$$

From (35), we observe that the diversity order is equal to the minimum of the product of the number of source and relay antennas and the first hop Nakagami- m fading parameter and the product of the number of relay and destination antennas and the second hop Nakagami- m fading parameter, which means the diversity order is entirely determined by the weaker hop. It also shows that the diversity order is only determined by the antenna configuration and Nakagami- m fading parameter and is independent of the correlation.

Numerical results

In this section, the theoretical analysis developed in the previous sections is validated via numerical examples, and we also compare the performance of the CSI-assisted relaying system with that of the fixed gain relaying system [29]. We consider doubly-correlated Nakagami- m fading channels. Without loss of generality, the exponential correlation model is adopted, where the correlation model at both transmitting and receiving ends of both hops are assumed to be identical. For exponential correlation model, the components of the correlation matrix can be given by [17,30-32]

$$\rho_{ij} = \rho^{|i-j|}, \quad 0 \leq \rho \leq 1, \quad (37)$$

where ρ is the correlation coefficient of the neighboring antennas. Obviously, (37) may be not an accurate model for some real-world scenarios but this is a simple single-parameter model which allows us to study the effect of correlation on the MIMO relaying system in an explicit way and to get some insight. And this model is physically reasonable in the sense that the correlation between a pair of signals decreases as the separation between them increases.

Figure 2 plots the PDF of the received end-to-end SNR γ for different terminal antenna configurations with different correlation coefficient ρ . It is observed that the analysis results of (20) match perfectly with the simulation results. The higher the correlation, the lower the end-to-end SNR. This phenomenon is more significant for system with larger number of antennas. It also shows that the end-to-end SNR γ with $\beta = 1$ can be tightly upper bounded

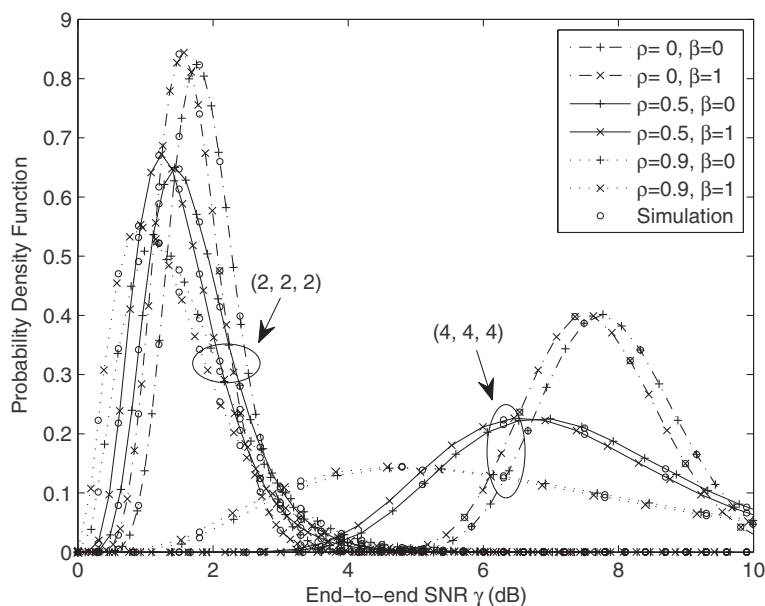


Figure 2 PDF of the end-to-end SNR γ for different terminal antenna configurations (N_S, N_R, N_D) . ($m_1 = m_2 = 2, \rho_1 = \rho_2 = 1, \bar{\gamma}_{1,j} = \bar{\gamma}_{2,j} = 1, R_{c,1} = R_{c,2} = 1$).

by γ with $\beta = 0$, which is consistent with (9). For brevity, we consider only the end-to-end SNR γ with $\beta = 0$ in the following.

Figures 3 and 4 depict the system outage probabilities variation with different antenna configurations and different correlation coefficients ρ with a threshold value $\gamma_{th} =$

10 dB. Figures 5 and 6 show the BER of BPSK modulation with different correlation coefficients ρ . As expected, the comparison shows an excellent agreement between analytical and simulation results, which validates the accuracy of our analytical results. The correlation deteriorates the OP and BER and the larger number of antennas improves

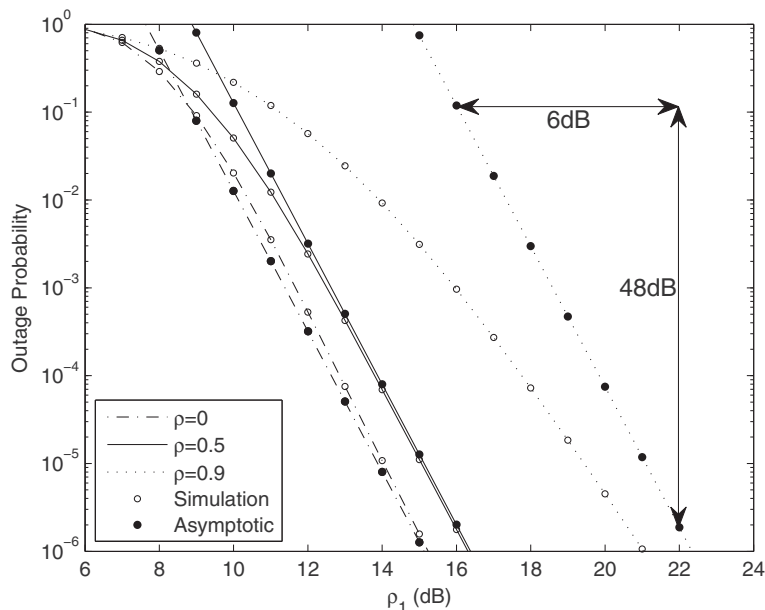


Figure 3 OP of the AF MIMO relaying system for a threshold $\gamma_{th} = 10$ dB with terminal antenna configuration $(N_S, N_R, N_D) = (2, 2, 2)$. ($m_1 = m_2 = 2, \kappa = 1, \bar{\gamma}_{1,j} = \bar{\gamma}_{2,j} = 1, R_{c,1} = R_{c,2} = 1$).

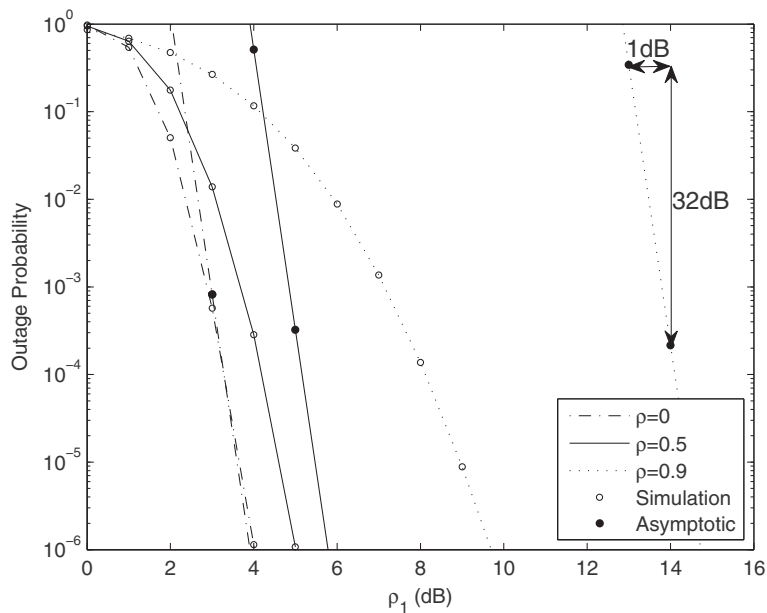


Figure 4 OP of the AF MIMO relaying system for a threshold $\gamma_{th} = 10$ dB with terminal antenna configuration $(N_S, N_R, N_D) = (4, 4, 4)$. ($m_1 = m_2 = 2, \kappa = 1, \bar{\gamma}_{1,j} = \bar{\gamma}_{2,j} = 1, R_{c,1} = R_{c,2} = 1$).

the OP and BER. From Figures 3, 4, 5 and 6, it can be concluded that the effect of correlation could be negligible when the correlation between two adjacent antennas are less than 0.5 but it becomes significant for $\rho > 0.5$, which is in agreement with previous results on the effect of spatial correlation [31,32].

The asymptotic results are also drawn in the Figures 3, 4, 5 and 6. The asymptotic curves in each figure are parallel, i.e., they have the same slope, but are shifted to the right as ρ increases from 0 to 0.9, which implies that the correlation has no impact on the achievable diversity order. This is consistent with the works in [7,15]. The asymptotic

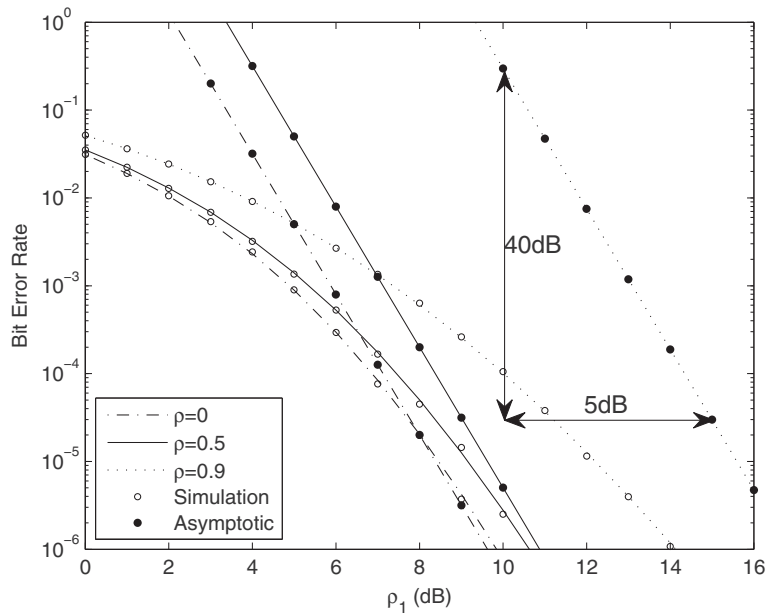


Figure 5 Bit error rate of BPSK for AF MIMO relaying systems with terminal antenna configuration $(N_S, N_R, N_D) = (2, 2, 2)$. ($m_1 = m_2 = 2, \kappa = 1, \bar{\gamma}_{1,j} = \bar{\gamma}_{2,j} = 1, R_{c,1} = R_{c,2} = 1$).

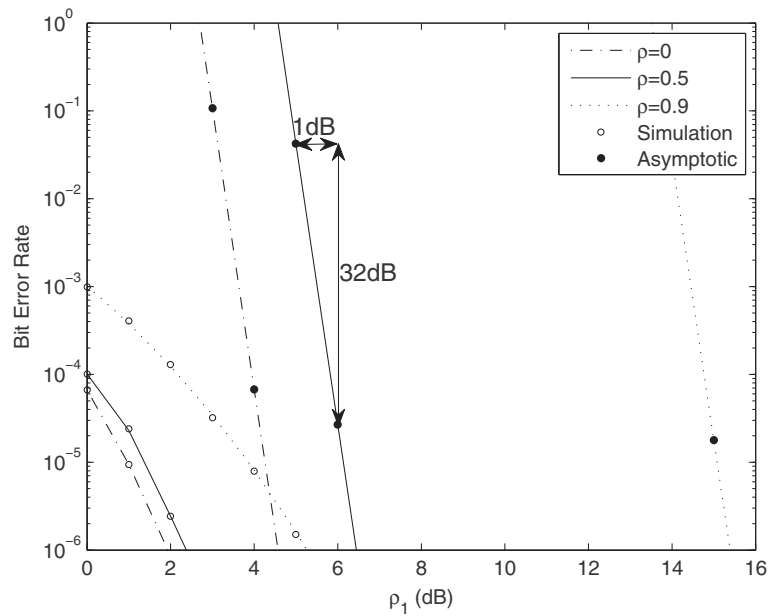


Figure 6 Bit error rate of BPSK for AF MIMO relaying systems with terminal antenna configuration $(N_S, N_R, N_D) = (4, 4, 4)$. ($m_1 = m_2 = 2$, $\kappa = 1, \bar{\gamma}_{1,j} = \bar{\gamma}_{2,j} = 1, R_{c,1} = R_{c,2} = 1$).

curves in Figures 3 and 5 are linear with a slope of 8, whereas the asymptotic curves in Figures 4 and 6 are very steep with a slope of 32. These observations agree with the result in Section “Symbol error rate”, namely, the diversity order is $\min\{\tilde{m}_1, \tilde{m}_2\}$.

Figure 7 plots the BER of CSI-assisted and fixed gain relaying systems with different correlation coefficients. It’s shown that the performance of fixed gain relaying system deteriorates seriously, especially for high correlation coefficient, which means that fixed gain relaying

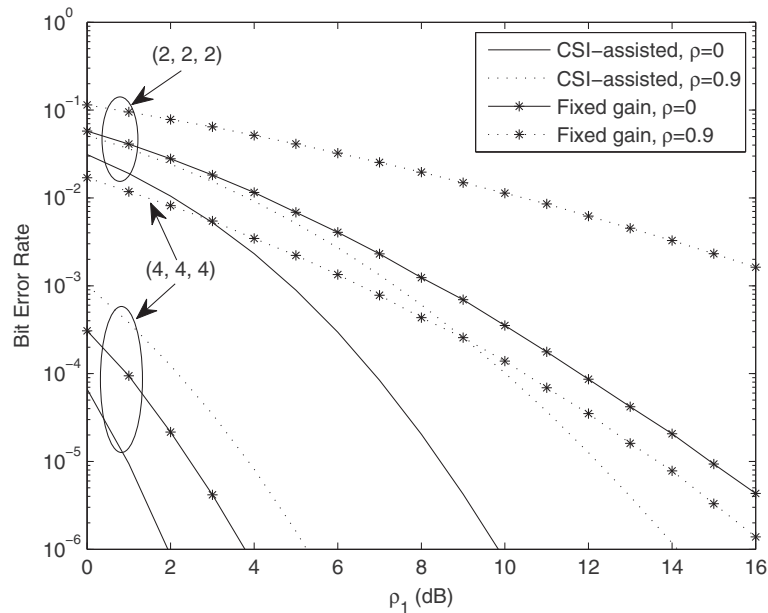


Figure 7 Comparison of BER of CSI-assisted and fixed gain relaying systems for different terminal antenna configurations (N_S, N_R, N_D) . ($m_1 = m_2 = 2, \kappa = 1, \bar{\gamma}_{1,j} = \bar{\gamma}_{2,j} = 1, R_{c,1} = R_{c,2} = 1$).

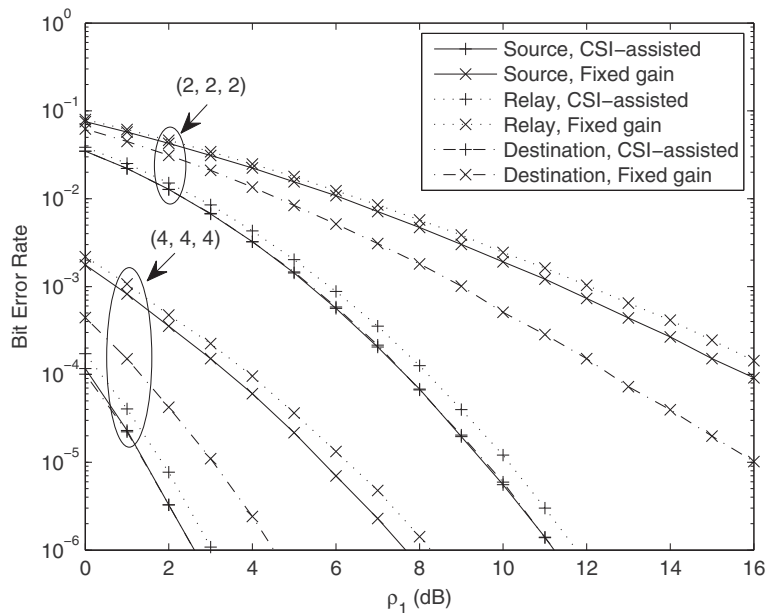


Figure 8 Comparison of BER of CSI-assisted and fixed gain relaying systems when correlation exists only at one terminal. ($m_1 = m_2 = 2$, $\kappa = 1$, $\bar{\gamma}_{1,j} = \bar{\gamma}_{2,j} = 1$, $R_{c,1} = R_{c,2} = 1$, $\rho = 0.9$).

system is much more influenced by the correlation than CSI-assisted relaying system.

Figure 8 compares the BER of CSI-assisted and fixed gain relaying systems when correlation exists only at one terminal with $\rho = 0.9$. Terms “source”, “relay”, and “destination” in the legend mean that correlation exists only at the source, relay, and destination, respectively.

For CSI-assisted relaying system, the performance of correlation at source and destination is almost the same, which is better than that of correlation at relay. This can be explained by the fact that the correlation at relay has negative influence on both hops, whereas correlation at source or destination has negative influence only on single hop. For fixed gain relaying system, the performance

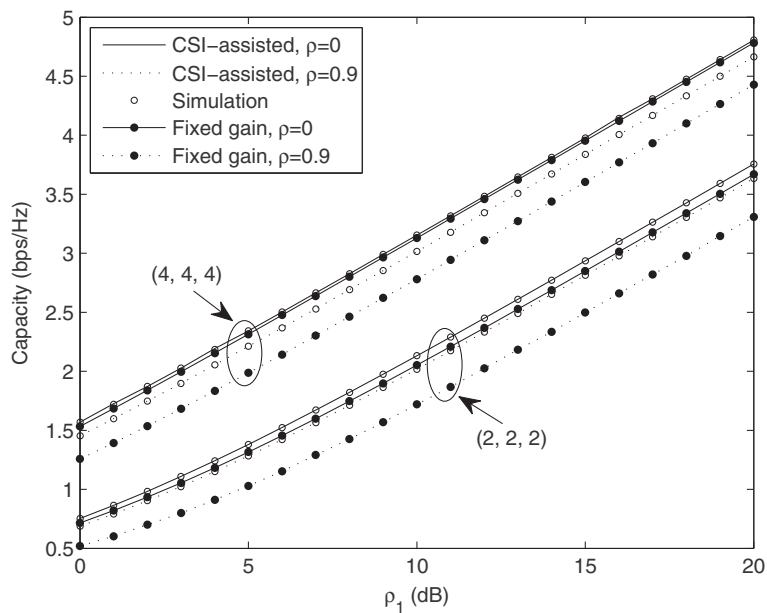


Figure 9 Comparison of ergodic capacity of CSI-assisted and fixed gain relaying systems. ($m_1 = m_2 = 2$, $\kappa = 1$, $\bar{\gamma}_{1,j} = \bar{\gamma}_{2,j} = 1$, $R_{c,1} = R_{c,2} = 1$).

of correlation at relay is worst. The performance of correlation at source is inferior to that of correlation at destination, and the gap between them is relatively large. The reason is that fixed gain relaying does not take the CSI of the first hop into account and the error in first hop has a dominant influence.

Comparison of ergodic capacity of CSI-assisted and fixed gain relaying systems is shown in Figure 9. Both approximate solution (29) and simulation results are plotted. It's observed that the CSI-assisted relaying system has a higher capacity, and this phenomenon is not obvious for independent channel fading ($\rho = 0$). The capacity is higher for high SNR, and becomes lower at higher correlation values. It is also shown that the closed-form approximation matches the simulation results very well, which verifies the accuracy of the approximation solution (29).

Conclusions

In this article, the performance of dual-hop AF MIMO relaying system with OSTBC transmissions over doubly-correlated Nakagami- m fading channel has been investigated. The compact closed-form expressions for CDF, PDF, MGF, and GM of the end-to-end SNR are derived. Besides, the exact analytical expressions for OP and SER and approximate expression for ergodic capacity are also derived. In order to gain more insight into system performance, we present the asymptotic expression for OP and SER in the high SNR regime, and derive the achievable diversity order and array gain of the AF MIMO relaying system. The analytical expressions have been analytically proved and verified through extensive simulations. All the cases investigated reveal an excellent agreement between the results from analysis and simulation. It is observed that system performance increases with the decrease of antenna correlation and the increase of antenna number. Furthermore, we compare the performance of CSI-assisted and fixed gain relaying systems in terms of BER and ergodic capacity. CSI-assisted relaying outperforms fixed gain relaying at the cost of complexity.

Appendices

Appendix 1

From [6], the CDF of end-to-end SNR γ expressed by (9) could be derived as

$$F_\gamma(\gamma) = 1 - \int_0^\infty P(\gamma_1 \geq \tilde{x} | x + \gamma) f_{\gamma_2}(x + \gamma) dx \quad (38)$$

where $\tilde{x} = (x + \gamma + \beta) \gamma / x$. From (17) and (18), we have

$$f_{\gamma_2}(x + \gamma) = \sum_{p=1}^{J_2} \sum_{q=1}^{m_2 v_{2,p}} \frac{c_{p,q}^2}{\Gamma(q)} \left(\frac{m_2}{\rho_2 \lambda_{2,p}} \right)^q (x + \gamma)^{q-1} \times \exp\left(-\frac{m_2}{\rho_2 \lambda_{2,p}} (x + \gamma)\right), \quad (39)$$

$$P(\gamma_1 \geq \tilde{x} | x + \gamma) = \sum_{j=1}^{J_1} \sum_{k=1}^{m_1 v_{1,j}} \sum_{l=0}^{k-1} \frac{c_{j,k}^1}{l!} \left(\frac{m_1 \tilde{x}}{\rho_1 \lambda_{1,j}} \right)^l \times \exp\left(-\frac{m_1 \tilde{x}}{\rho_1 \lambda_{1,j}}\right). \quad (40)$$

Substituting (39) and (40) into (38), and performing some algebraic manipulations, with the help of definite integral of exponential function, given by ([21], eq. (3.471.9)), and the binomial theorem, given by ([21], eq. (1.111)), the closed-form expression for the CDF can be derived as shown in (19).

Appendix 2

MGF $\mathcal{M}_\gamma(s)$ associates with the fading PDF $f_\gamma(\gamma)$ and is defined by [24]

$$\mathcal{M}_\gamma(s) = \int_0^\infty e^{-s\gamma} f_\gamma(\gamma) d\gamma = 1 - s \int_0^\infty e^{-s\gamma} (1 - F_\gamma(\gamma)) d\gamma \quad (41)$$

Substituting (19) into (41) yields

$$\mathcal{M}_\gamma(s) = 1 - 2s \sum_{j=1}^{J_1} \sum_{k=1}^{m_1 v_{1,j}} \sum_{l=0}^{k-1} \sum_{p=1}^{J_2} \sum_{q=1}^{m_2 v_{2,p}} \sum_{g=0}^{l} \sum_{h=0}^{l-g} \binom{q-1}{g} \binom{l}{h} \times \frac{c_{j,k}^1 c_{p,q}^2}{\Gamma(l+1) \Gamma(q)} \left(\frac{m_1}{\rho_1 \lambda_{1,j}} \right)^{\frac{\theta+1}{2}} \left(\frac{\rho_2 \lambda_{2,p}}{m_2} \right)^{\frac{\theta-l}{2}-q} \times \sum_{\mu=0}^{g+l+2} \binom{g+l+2}{\mu} \beta^{g+l-\mu+2} \Delta, \quad (42)$$

where

$$\Delta = \gamma^{q-g+\mu-1} \int_0^\infty \exp\left(-\left(s + \frac{m_1}{\rho_1 \lambda_{1,j}} + \frac{m_2}{\rho_2 \lambda_{2,p}}\right) \gamma\right) \times \gamma^{\frac{\theta+l}{2}} (\gamma + \beta)^{-\frac{\theta+l+2}{2}} K_{\theta-l} \left(2 \sqrt{\frac{m_1 m_2 \gamma (\gamma + \beta)}{\rho_1 \lambda_{1,j} \rho_2 \lambda_{2,p}}} \right) d\gamma = \frac{\Gamma(\theta+1) \Gamma(l+1)}{2\beta^{\theta+l+2} (-1)^{q-g+\mu-1}} \left(\frac{m_1 m_2}{\rho_1 \lambda_{1,j} \rho_2 \lambda_{2,p}} \right)^{-\frac{\theta+l+2}{2}} \times \frac{d^{q-g+\mu-1}}{d\tilde{s}^{q-g+\mu-1}} ({}_2F_0(\theta+1, l+1; -; -\omega(\tilde{s} + \tilde{s}')) \times {}_2F_0(\theta+1, l+1; -; -\omega(\tilde{s} - \tilde{s}')))|_{\tilde{s}=s}. \quad (43)$$

It is deduced by performing some algebraic manipulations using the identities for Laplace transformation, given in ([22], eqs. (4.17.20) and (4.1.6)), and the relationship between Whittaker functions and generalized hypergeometric functions, given in [33]. Substituting (43) into (42) gives (21).

Competing interests

The authors declare that they have no competing interests.

Author details

¹Research & Innovation Center, Alcatel-Lucent Shanghai Bell Co. Ltd., Shanghai, China. ²School of Information and Electronics, Beijing Institute of Technology, Beijing, China.

Received: 1 April 2012 Accepted: 17 July 2012

Published: 18 September 2012

References

- JN Laneman, DNC Tse, GW Wornell, Cooperative diversity in wireless networks: efficient protocols and outage behavior. *IEEE Trans. Inf. Theory.* **50**(12), pp. 3062–3080 (2004)
- MO Hasna, M-S Alouini, End-to-end performance of transmission systems with relays over Rayleigh-fading channels. *IEEE Trans. Wirel. Commun.* **2**(6), pp. 1126–1131 (2003)
- MO Hasna, M-S Alouini, A performance study of dual-hop transmissions with fixed gain relays. *IEEE Trans. Wirel. Commun.* **3**(6), pp. 1963–1968 (2004)
- C Hoymann, W Chen, J Montojo, A Golitschek, C Koutsimanis, X Shen, Relaying operation in 3GPP, LTE: challenges and solutions. *IEEE Commun. Mag.* **50**(2), pp. 156–162 (2012)
- D Senaratne, C Tellambura, Unified exact performance analysis of two-hop amplify-and-forward relaying in Nakagami fading. *IEEE Trans. Veh. Technol.* **59**(3), pp. 1529–1534 (2010)
- RHY Louie, Y Li, HA Suraweera, B Vucetic, Performance analysis of beamforming in two hop amplify and forward relay networks with antenna correlation. *IEEE Trans. Wirel. Commun.* **8**(6), pp. 3132–3141 (2009)
- NS Ferdinand, N Rajatheva, Unified performance analysis of two-hop amplify-and-forward relay systems with antenna correlation. *IEEE Trans. Wirel. Commun.* **10**(9), pp. 3002–3011 (2011)
- HA Suraweera, HK Garg, A Nallanathan, Beamforming in dual-hop fixed gain relay systems with antenna correlation, in *Proc. IEEE ICC*, May 2010
- DB da Costa, S Aissa, Cooperative dual-hop relaying systems with beamforming over Nakagami- m fading channels. *IEEE Trans. Wirel. Commun.* **8**(8), pp. 3950–3954 (2009)
- N Yang, M Elkashlan, J Yuan, T Shen, On the SER of fixed gain amplify-and-forward relaying with beamforming in Nakagami- m fading. *IEEE Commun. Lett.* **14**(10), pp. 942–944 (2010)
- I-H Lee, D Kim, End-to-end BER analysis for dual-hop OSTBC transmissions over Rayleigh fading channels. *IEEE Trans. Commun.* **56**(3), pp. 347–351 (2008)
- TQ Duong, H-J Zepernick, TA Tsiftsis, VNQ Bao, Amplify-and-forward MIMO relaying with OSTBC over Nakagami- m fading channels, in *Proc. IEEE ICC*, May 2010
- L Yang, QT Zhang, Performance analysis of MIMO relay wireless networks with orthogonal STBC. *IEEE Trans. Veh. Technol.* **59**(7), pp. 3668–3674 (2010)
- NS Ferdinand, N Rajatheva, M Latva-aho, Effects of antenna correlation in MIMO two hop AF relay network over Rayleigh-Rician channels. *IEEE Commun. Lett.* **15**(9), pp. 941–943 (2011)
- TQ Duong, GC Alexandropoulos, H-J Zepernick, TA Tsiftsis, Orthogonal space-time block codes with CSI-assisted amplify-and-forward relaying in correlated Nakagami- m fading channels. *IEEE Trans. Veh. Technol.* **60**(3), pp. 882–889 (2011)
- R Janaswamy, *Radiowave Propagation and Smart Antennas for Wireless Communications*. (Kluwer Academic Publishers, Boston, 2000)
- H Shin, MZ Win, JH Lee, M Chiani, On the capacity of doubly correlated MIMO channels. *IEEE Trans. Wirel. Commun.* **5**(8), pp. 2253–2265 (2006)
- P Lombardo, G Fedele, MM Rao, MRC performance for binary signals in Nakagami fading with general branch correlation. *IEEE Trans. Commun.* **47**(1), pp. 44–52 (1999)
- X Li, T Luo, G Yue, C Yin, A squaring method to simplify the decoding of orthogonal space-time block codes. *IEEE Trans. Commun.* **49**(10), pp. 1700–1703 (2001)
- C-N Chuah, DNC Tse, JM Kahn, RA Valenzuela, Capacity scaling in MIMO wireless systems under correlated fading. *IEEE Trans. Inf. Theory.* **48**(3), pp. 637–650 (2002)
- IS Gradshteyn, IM Ryzhik, *Table of Integrals, Series, and Products*, 7th ed, (Academic, San Diego, CA, 2007)
- A Erdelyi, W Magnus, F Oberhettinger, FG Tricomi, vol 1, (McGraw-Hill, New York, 1954)
- YA Brychkov, *Handbook of Special Functions: Derivatives, Integrals, Series and Other Formulas*, (CRC Press, Moscow, 2008)
- MK Simon, M-S Alouini, *Digital Communication Over Fading Channels: A Unified Approach to Performance Analysis*, (Wiley, New York, 2000)
- MR McKay, AJ Grant, IB Collings, Performance analysis of MIMO-MRC in double-correlated Rayleigh environments. *IEEE Trans. Commun.* **55**(3), pp. 497–507 (2007)
- DB da Costa, S Aissa, Capacity analysis of cooperative systems with relay selection in Nakagami- m fading. *IEEE Commun. Lett.* **13**(9), pp. 637–639 (2009)
- Z Fang, L Li, Z Wang, Asymptotic performance analysis of multihop relayed transmissions over Nakagami- m fading channels. *IEICE Trans. Commun.* **E91-B**(12), pp. 4081–4084 (2008)
- Z Wang, GB Giannakis, A simple general parameterization quantifying performance in fading channels. *IEEE Trans. Commun.* **51**(8), pp. 1389–1398 (2003)
- P Dharmawansa, MR McKay, RK Mallik, Analytical performance of amplify-and-forward MIMO relaying with orthogonal space-time block codes. *IEEE Trans. Commun.* **58**(7), pp. 2147–2158 (2010)
- VA Aalo, Performance of maximal-ratio diversity systems in a correlated Nakagami- m fading environment. *IEEE Trans. Commun.* **43**(8), pp. 2360–2369 (1995)
- SL Loyka, Channel capacity of MIMO architecture using the exponential correlation matrix. *IEEE Commun. Lett.* **5**(9), pp. 369–371 (2001)
- M Chiani, MZ Win, A Zanella, On the capacity of spatially correlated MIMO Rayleigh-fading channels. *IEEE Trans. Inf. Theory.* **49**(10), pp. 2363–2371 (2003)
- HJ Silverstone, S Nakai, JG Harris, Observations on the summability of confluent hypergeometric functions and on semiclassical quantum mechanics. *Phys. Rev. A.* **32**(3), pp. 1341–1345 (1985)

doi:10.1186/1687-1499-2012-294

Cite this article as: Yang et al.: Dual-hop MIMO relaying with OSTBC over doubly-correlated Nakagami- m fading channels. *EURASIP Journal on Wireless Communications and Networking* 2012 **2012**:294.

Submit your manuscript to a SpringerOpen® journal and benefit from:

- Convenient online submission
- Rigorous peer review
- Immediate publication on acceptance
- Open access: articles freely available online
- High visibility within the field
- Retaining the copyright to your article

Submit your next manuscript at ► springeropen.com